Contextualizing yellow light-emitting electrochemical cells based on a blue-emitting imidazo-pyridine emitter

Contextualizing yellow light-emitting electrochemical cells based on a blue-emitting imidazo-pyridine emitter

E. Fresta[a], G. Volpi[b], C. Garino[b], C. Barolo[b,c]*, R. D. Costa[a]*

[a]*IMDEA Materials Institute, Calle Eric Kandel 2, 28906 Getafe, Madrid, Spain*
[b]*Department of Chemistry, NIS Interdepartmental Centre and INSTM Reference Centre, Università degli Studi di Torino, Via Pietro Giuria 7, 10125 - Torino, Italy*
[c]*ICxT Interdepartmental Centre, Università degli Studi di Torino, Lungo Dora Siena 100, 10153 - Torino, Italy*
* corresponding author claudia.barolo@unito.it, ruben.costa@imdea.org

Keywords: Light-emitting electrochemical cells, Blue-emission, Small molecules, Pyridilimidazo[1,5-a]pyridine, Aggregation

Abstract

This work provides the synthesis, structural characterization, electrochemical and photophysical features, as well as the application in light-emitting electrochemical cells (LECs) of a novel small molecule belonging to the pyridilimidazo[1,5-a]pyridine family, namely 3-(2-methoxyphenyl)-5-methyl-1-(6-methylpyridin-2-yl)H-imidazo[1,5-a]pyridine (Me-impy). This compound shows a low-cost and facile synthesis, excellent redox properties, and a high photoluminescence quantum yield (Φ) of 0.4 associated to a blue emission (~436 nm) in solution. Despite these appealing features, the emission in solid state is red-shifted to the yellow region, owing to its prone aggregation character. Additionally, the electroluminescence response shows a broader and red-shifted emission even upon dilution of Me-impy thin films with polymethyl methacrylate (PMMA). Herein, we report an in-depth study on the aggregation features and its impact on the electroluminescence response of Me-impy, providing relevant information to design small-molecule based LECs.

1. Introduction

Light-emitting electrochemical cells (LECs) are regarded as one of the most promising thin-film lighting sources, as they combine high efficiency, a simple architecture with air stable electrodes, and a low-cost, solution based up-scalable fabrication process [1–4]. In short, LECs are a single-layer electroluminescent device consisting of a mixture of a luminescent material and an ionic electrolyte. As such, the main difference from the well-established organic light-emitting diode (OLED) technology is the control of the charge injection using mobile ions [5]. Upon biasing the device, the ion redistribution towards the electrode interface assists the electrochemical doping forming a p-i-n junction structure [3,6–13]. This particular operational mode leads to a high tolerance towards (i) working function of the electrodes paving the way of using air-stable cathodes, such as Ag or Al, (ii) different thicknesses and minor defects of the active layer, (iii) using low-cost and up-scalable solution based techniques, and (iv) applying a huge palette of emitters, such as polymers, ionic transition metal complexes, small molecules, quantum dots, and perovskites [2,14–22].

The future advances in the field head into two directions, namely (i) the development of new device architectures, such as flexible and/or 3D shaped substrates based on metallic and/or semiconducting materials, and (ii) new low-cost, easily synthetisable, and sustainable luminescent materials spanning the whole visible range [1–3,23]. As far as the first aspect is concerned, LECs fabricated with industry relevant based techniques, such as inkjet printing [24], roll-to-roll-coating [25], spray-coating [26], and slot-die coating [25], have been reported, as well as wearable fiber-shaped devices [27,28]. Regarding the new generation of emitters, small molecules have recently attracted much attention, due to (i) their wide variety using easily modifiable scaffolds, (ii) their emission covering the whole visible range with high U values that are not subjected to ambient quenching, (iii) their stable electrochemical and thermal features, (iv) their easy processability and high stability in solution, (v) their good carrier mobilities, and (vi) the presence of a thermally activated delayed fluorescence (TADF) behavior [3,29–34].

Numerous works have been reported in the last few years regarding various families of small molecules for LECs (hereafter abbreviated as SM-LECs), such as ionic fluorine derivatives, phenanthroimidazoles, borazines, carbazoles, benzodithiazoles, pyrene derivatives, porphyrins, pentacenes, and cyanines [16,29,35–47]; covering all the visible spectrum including white emission [14,15]. Concerning blue SM-LECs, only three main families, namely ionic fluorine derivatives, imidazoles and borazines, have been tested [29,31,35–37,39,40,48,49]. Moderate efficiencies of 0.18 cd/A were reported by Choe et al., along with a maximum luminance of 711 cd/m^2 under L-I-V assays [39]. However, stability still remains a bottleneck, highlighting that many efforts still have to be done in the field.

In order to widen the horizon of candidates for blue SM-LECs, we focused our attention on a pyridilimidazo[1,5-a]pyridine (impy), namely 3-(2-methoxyphenyl)-5-methyl-1-(6-methylpyridin-2-yl)H-imidazo[1,5-a]pyridine), referred to as Me-impy in the work at hand – Fig. 1. Pyridilimidazo[1,5-a]pyridines have found applications mainly as diamine (N^N) ligands in a large variety of fields, including organic thin-layer field effect transistors (OFETs) [50], LEDs [51], and OLEDs [52]. The wide interest is fueled by (i) low-cost, facile, and high-yield synthesis, (ii) blue emission centered around 430 nm with high / values, (iii) excellent solution stability, and (iv) reversible electrochemical features [53–57]. Although this family of blue emitters can be, at a first glance, regarded as appealing candidates for SM-LECs, their electroluminescent features in LECs have been counterintuitive up to date [58]. For instance, LECs based on a blue emitting heteroleptic [Cu(impy)(POP)]PF_6 complex, in which POP is bis(2-(diphenylphosphanyl)phenyl) ether – Fig. 1, showed a yellow electroluminescent response due to the absence of an effective TADF process, leaving the triplet excited state as the only radiative deactivation pathway under electrical stimuli [58]. This is, indeed, rather surprising in this type of emitters [34,59–62].

All of the aforementioned has encouraged us to further investigate the inherent electroluminescent properties of Me-impy. Despite the excellent blue emitting features, yellowish LECs were obtained due to its prone aggregation behavior in thin films. Strikingly enough, the best performing devices with Me-impy showed,

however, similar figures-of-merit that devices prepared with either copper(I) or iridium(III) complexes bearing Me-impy as ancillary N^N ligand – i.e., $[Ir(ppy)_2(Me\text{-}impy)]PF_6$ where ppy is phenylpyridine and $[Cu(impy)(POP)]PF_6$ as shown in Fig. 1. As such, this work contextualizes the unforeseen electroluminescent behavior of pyridilimidazo[1,5-a]pyridine emitters employed in LECs, providing relevant information to develop new candidates for SM-LECs.

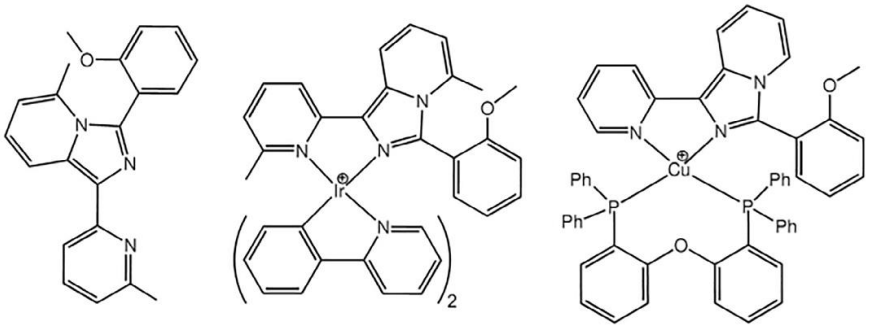

Fig. 1. Chemical structures of Me-impy (left), $[Ir(ppy)_2(Me\text{-}impy)]^+$ (middle), and $[Cu(impy)(POP)]^+$ (right).

2. Experimental details

2.1 Synthesis

All chemicals were purchased fromchemical suppliers and used without further purification. All analytical reagent grade solvents were purified by distillation. All reactions were carried out under inert nitrogen atmosphere using standard vacuum lines techniques. ^{1}H- and ^{13}C NMR spectra were recorded on a Bruker Avance 200 spectrometer (^{1}H NMR operating frequency 200 MHz) and on a JEOL ECP 400 spectrometer (^{1}H NMR operating frequency 400 MHz), with chemical shifts referenced to residual protons of the solvent. The following abbreviations are used: s, singlet; d, doublet; t, triplet; m, multiplet. Mass spectra were recorded using a Thermo-Finnigan Advantage Max Ion Trap Spectrometerequipped with an electrospray ion source (ESI).

2,2'-dimethyldipyridilketone

In a 50 mL round-bottomed flask containing 15 mL dry tetrahydrofuran solution of 2-bromopyridine (0.79 g, 5 mmol), 3 mmol (0.19 g) of n-butyl lithium (2.5 M in hexane) was added over 20 min at –78 °C under N_2 and the resulting mixture was stirred at –78 °C for 5 min. The addition of 10 mmol (1.18 g) of diethyl carbonate followed. The mixture was warmed to room temperature and quenched with HCl 10% until acidic. The mixture was then basified with a saturated solution of Na_2CO_3 in water and extracted 3 times with dichloromethane (DCM), anhydrificated and dried, giving yield to a yellow/orange oil. The oil was purified via flash column chromatography using a mixture of DCM and methanol (MeOH) in a ratio of 96:4, giving yield to the desired 2,2'-Dimethyldipyridilketone. ^{1}H NMR (200 MHz, $CDCl_3$): d 2.62 (s, 6H), 7.33 (d, J = 7.6, 2H), 7.74 (m, 2H), 7.79 (d, J = 7.6, 2H) ppm. ^{13}C NMR (50 MHz, $CDCl_3$): d 24.6, 123.0, 126.1, 136.6, 153.6, 158.3, 193.3 ppm. *m/z* (ESI+) for $C_{13}H_{13}N_2O$ calcd 213.10 $[M+H]^+$, found 212.98 $[M+H]^+$.

3-(2-methoxyphenyl)-5-methyl-1-(6-methylpyridin-2-yl)H-imidazo[1,5-a]pyridine

3 mmol of 2,2'-dimethyldipyridilkethone (0.65 g) was mixed with 2-methoxybenzaldehyde (0.61 g, 4.5 mmol) and ammonium acetate NH_4OAc (1.15 g, 15 mmol) in glacial acetic acid HOAc (15 mL). The solution was stirred at 110 °C under inert atmosphere. After 5 h, the reaction mixture was cooled to room temperature and the acetic acid was removed by evaporation under reduced pressure. The obtained solid was dissolved in a saturated aqueous solution of Na_2CO_3 and the mixture extracted with DCM. The organic layer was separated, dried and the solvent evaporated under vacuum. The obtained crude product (yellow-orange solid, 0.91 g, yield 93%) was purified via column chromatography on silica gel (DCM:MeOH 98:2). ^{1}H NMR (200 MHz, Acetone-d6) 2.15 (s, 3H), 2.58 (s, 3H), 3.75 (s, 3H), 6.46 (d, J = 6.9 Hz, 1H), 6.88 (dd, J =

6.5, 2.7, 1H), 6.97 (d, J = 9.1 Hz, 1H) 7.03–7.13(m, 2H), 7.49–7.60 (m, 3H) 7.97 (d, J = 9.6 Hz, 1H), d 8.79 (d, J = 9.8 Hz, 1H) ppm. ^{13}C NMR (50 MHz, Acetone-d6): d 19.76, 20.28, 55.72, 111.40, 111.74, 117.20, 120.05, 124.72, 129.95, 131.85, 131.92, 133.52, 134.68, 136.45, 137.17, 155.96, 157.95, 159.77 ppm. *m/z* (ESI+) for $C_{21}H_{20}N_3O$ calcd 330.16 $[M+H]^+$, found 330.21 $[M+H]^+$.

2.4. $[Ir(ppy)_2(Me\text{-}impy)]PF_6$

The iridium(III) complex $[Ir(ppy)_2(Me\text{-}impy)]PF_6$ was synthesized following standard procedures reported in literature [63–65]. ^{1}H NMR (400 MHz, Acetone-d6): d 2.42 (s, 3H), 2.55 (s, 3H), 3.58 (s, 3H), 5.64 (d, J = 7.25, 1H), 6.17 (d, J = 7.52, 1H), 6.32 (d, J = 7.38, 1H), 6.38 (t, J = 7.38, 1H), 6.45 (d, J = 7.46, 1H), 6.52 (m, 2H), 6.68 (m, 2H), 6.82 (m, 2H), 7.15 (m, 2H), 7.21 (m, 2H), 7.30 (d, J = 8.86, 1H), 7.34 (3, 1H), 7.67 (d, J = 8.06, 1H), 7.86 (d, J = 6.71, 1H), 7.96 (t, J = 8.19, 1H), 7.05 (m, 3H), 8.34 (d, J = 8.19, 1H), 8.40 (d, J = 9.40, 1H), 8.47 (d, J = 5.50, 1H) ppm. *m/z* (ESI+) for $C_{43}H_{35}N_5OIr$ calcd 830.25 $[M]^+$, found 830.32 $[M]^+$. Elemental analysis calcd (%) for $C_{43}H_{35}F_6IrN_5OP$: C 52.97, H 3.62, N 7.18; found: C 52.49, H 3.89, N 6.93.

2.5. Spectroscopic, electrochemical, and morphology characterization

Steady-state absorption spectra were recorded with a Perkin Elmer Lambda 35. Steady-state emission spectra were recorded with a Fluoromax spectrometer from HORIBA Jobin Yvon IBH by using fluorescence and phosphorescence mode (measurement after 10 ns). Atomic Force Microscope (AFM) assays were performed with VEECO DIMENSION 5000 with a NanoScope V probe head and the Gwyddion evaluation software. Cyclic voltammetry was performed with a Metrohm µAutolabIII/FRA3 potentiostat, in acetonitrile (MeCN) solution, using the redox couple Cp_2Fe/Cp_2Fe^+ as internal reference ($E_{1/2}$ = +0.40 V), a solution of tetrabutylammonium hexafluorophosphate 0.1 M as electrolyte and a glassy/carbon electrode as working electrode. The scan speed was of 100 mV/s.

2.6. Device fabrication and analysis

ITO substrates were purchased from Naranjo Substrates with an ITO thickness of 130 nm. They were firstly cleaned with detergent, water, ethanol, and propan-2-ol as solvents in an ultrasonic bath (frequency 37–70 Hz, 30–40 °C) for 15 min each. Afterwards, the slides were dried with N_2 gas and put in an UV-ozone cleaner for 8 min. A solution of poly(3,4-ethylenedioxythiophene):poly(styrenesulfonate) (PEDOT:PSS) was filtered, sonicated and mixed with propan-2-ol in a ratio of 3:1. 50 µL of the aforementioned solution was dropped onto the ITO, while the spin coater was rotating at a speed of 1500 rpm for 60 s giving rise to a thickness of 70 nm after drying the covered substrates for 10 min at 120 °C. PEDOT:PSS (Clevios PAl4083) was purchased from Heraeus. The slides were then stored in a N_2-glovebox (O_2 level < 0.1 ppm, H_2O level < 0.5 ppm). Me-impy was dissolved in acetonitrile with a concentration of 15 mg/mL. It was stirred in a closed vial for 30 min and, if necessary, it was filtered. In order to obtain a thickness of around 100 nm of active layer, 75 µL of the solution was spread onto the substrate that was later on spin coated with a speed of 1000 rpm for 50 s. The coated slides were then transferred into N_2-glovebox and dried on a hotplate for 30 min at 90 °C. The active layer was deposited by spin-coating from a tetrahydrofuran (THF) solution of the Me-impy. In order to furnish the necessary ion mobility, a TMPE: LiOTf matrix was added, in the following ratio: Me-impy: TMPE:LiOTf 1:0.15:0.06. The thickness of the active layer was 100 nm. Two types of active layer were characterized, in which the ratio wt% Me-impy:PMMA was 1:0 (named 100 in this work) or 0.2:0.8 (20). The active layer of the LEC was prepared from an acetonitrile solution of the Ir(III) complex with the ionic liquid ethyl methyl imidazolium hexafluorophosphate ($[EMIM]PF_6$) in ratio 1:1, reaching a thickness of 120 nm. Once the active layer was deposited, the samples were transferred into an inert atmosphere glovebox (<0.1 ppm O_2 and H_2O, Innovative Technology). Aluminum cathode electrode (90 nm) was thermally evaporated using a shadow mask under high vacuum ($<1 \times 10^{-6}$ mbar) using an Angstrom Covap evaporator integrated into the inert atmosphere glovebox. Time dependence of luminance, voltage, and current was measured by applying constant and/or pulsed voltage and current by monitoring the desired parameters simultaneously by using Avantes spectrophotometer (Avaspec-ULS2048L-USB2) in conjunction

with a calibrated integrated sphere Avasphere 30-Irrad and Botest OLT OLED Lifetime-Test System. Electroluminescence spectra were recorded using the above mentioned spectrophotometer.

3. Results and discussion

3.1 Synthesis

The synthesis of Me-impy was performed in a two-step synthetic protocol reported elsewhere (Fig. 2) [53,65]. Its purity was confirmed by mass spectrometry, ^{1}H NMR, and ^{13}C NMR.

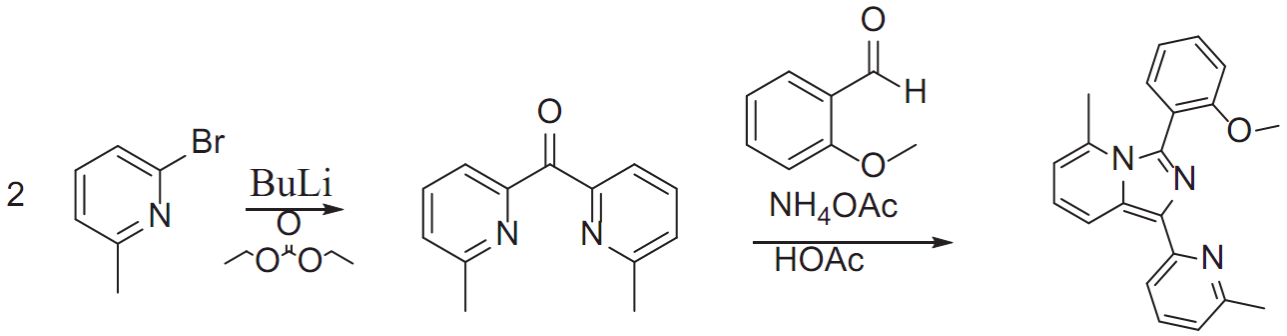

Fig. 2. Two step synthesis of Me-impy. (3-(2-methoxyphenyl)-5-methyl-1-(6-methylpyridin-2-yl)H-imidazo[1,5-a]pyridine).

3.2. Electrochemical characterization

As shown in Fig. 3 and summarized in Table 1, Me-impy shows two reversible oxidation waves located at 0.44 V and 0.85 V, while only one quasi-reversible reduction wave centred at –1.48 V was noted. Both oxidation and reduction are ascribed to the benzoimidazolic unit as supported by previous theoretical studies [53,54]. Thus, the charge and transport processes might be operative under device operative conditions.

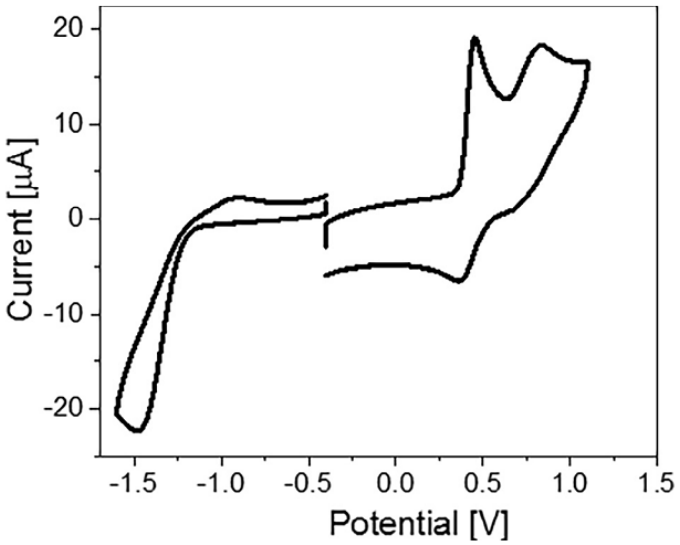

Fig. 3. Cyclic voltammogram of Me-impy in MeCN.

Table 1. Spectroscopic and electrochemical features of Me-impy.

Absorption			**Emission**					**Electrochemistry**	
Solution[a]	[ε]	Thin film	Solution	Powder		Thin film	Φ[a]	E_{ox} (V)[b]	E_{red} (V)[b]
λ_{max}(nm)	(10^5 $Lmol^{-1}cm^{-1}$)	λ_{max}(nm)	λ_{max}(nm) 298 K	λ_{max}(nm) 298 K	λ_{max}(nm) 77 K	λ_{max}(nm) 298K			
286, 335, 370	3.0	329, 370, 404 (shoulder)	436, 418, 464	435, 456	418, 430, 454	450 (lower), 559	0.39	$+0.44_{(r)}$ $+0.85_{(r)}$	$-1.46_{(r)}$

[a] Measured in MeCN.
[b]Measured with integrating sphere. λ_{exc} = 370 nm. b. qr = quasi reversible, r = reversible.

3.3. Spectroscopic characterization

Me-impy presents three main absorption peaks in MeCN located at 286, 330, and 367 nm each associated to a molar extinction coefficient of 30,000 mol^{-1} cm^{-1} – Fig. 4 and Table 1. These values are in line with the previously works on the family of emitters bearing the imidazo[1,5-a]pyridine moiety [53,54,63,66–68]. Concerning the photoluminescence features, Me-impy shows an emission maxima at 440 nm flanked by two shoulders at 418 and 463 nm – Fig. 4. The ϕ is around 0.4 in MeCN, underlying its potential as candidate for lighting applications. The photoluminescence parameters above are similar to those in powder – Figs. 4 and 5 as well as Table 1. The emission spectrum in powder consists of a broader and well-structured emission band featuring two maxima at 435 and 456 nm followed by two less intense bands at 489 and 556 nm. This indicates the presence of aggregates in the powder sample. Upon cooling up to 77 K, a more defined vibrational spectrum with three maxima at 417, 432 and 453 nm (shoulder) was noted. Fig. 5.

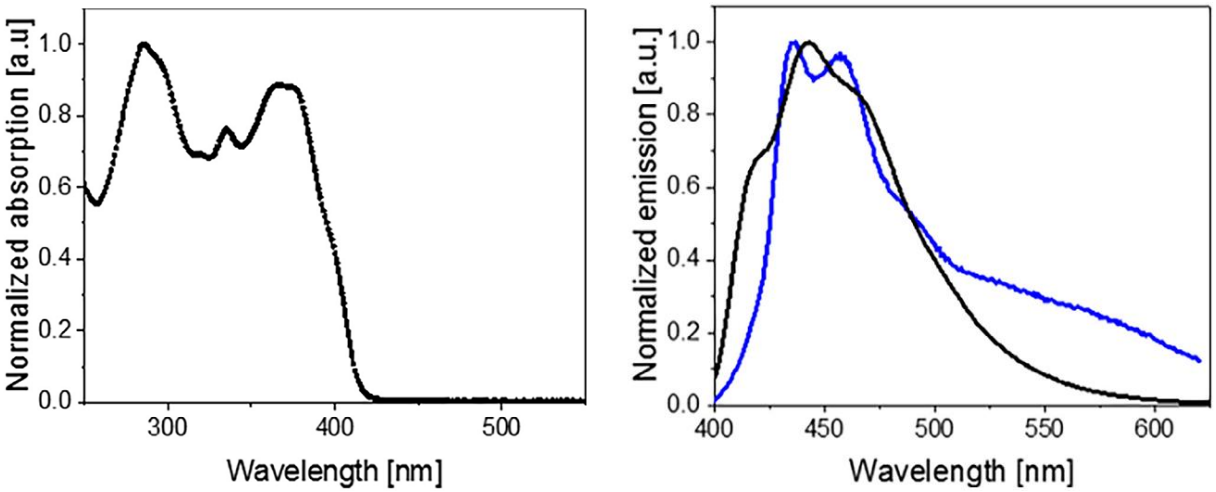

Fig. 4. Absorption (left) and photoluminescence (right) of Me-impy in MeCN (black line) and powder (blue line). (Colour online).

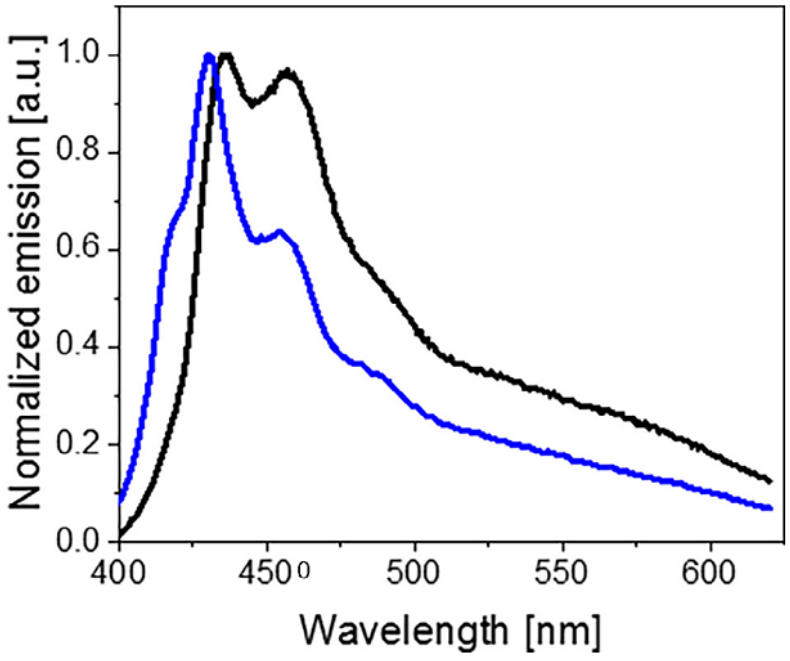

Fig. 5. Photoluminescence spectrum of Me-impy as powder at room temperature (black line) and at 77 K (blue line). (Colour online).

Next, we turned our attention to investigate the spectroscopic features of thin-films (100 nm) used for device fabrication, that is, a blend of Me-impy with ionic polyelectrolyte mixture – i.e. trimethylolpropane ethoxylate (TMPE): lithium triflate (LiOTf) ionic matrix in ratio 1:0.15:0.06 with Me-impy as 1. In contrast to both powder and solution emissions, these films show a yellowish emission with two maxima centered at 450 and 559 nmand x/y CIE of 0.34/0.40 – Fig. 6. While the high-energy emission peak is ascribed to the monomeric species of Me-impy, the latter should be ascribed to the presence of aggregates. This was confirmed by AFM characterization of the films. As shown in Fig. 6, the presence of aggregates with a size of ~200 nm and a height of 6–8 nm is clearly observed. The nature of these aggregates can be ascribed to π-π stacking interactions– Fig. 6. The stacking angles and the tridimensional arrangement are so far unknown and need further corroboration. As a second experiment, we prepared diluted films with different concentrations of polymethyl methacrylate or PMMA – i.e., 100:0, 80:20, 50:50, 20:80 wt.% Me-impy:PMMA hereafter abbreviated as **100**, **80**, **50** and **20** according to the wt% of Me-impy in the films – to reduce the formation of aggregates in the thin-film above – see experimental section for more details. Please notice that both PMMA and the ionic polyelectrolyte matrix show featureless absorption or emission spectra. As shown in Fig. 7, the absorption features of **100** films consist of two well-defined peaks at 330 nm and 366 nm in concert with two low-energy shoulders at around 400–425 nm. The latter are progressively disappearing upon diluting the emitter into the PMMA matrix. Indeed, the absorption spectrum of 20 and 50 films involve a well-defined band peaking at 310 nm, while spanning the range from 300 to 400 nm. Much more interesting is the photoluminescence features of the films above. In particular, while 20 and 50 films show performances of the evaporated devices, measured at the pulsed current of 15 mA approximately the same blue-emission features as in solution – Figs. 4 and 7, 80 films show a broad emission with two maxima 450 and 535 nm related to the monomer and aggregated species. Overall, both experiments indicate that the emission of thin films is ruled by both monomer and aggregate species.

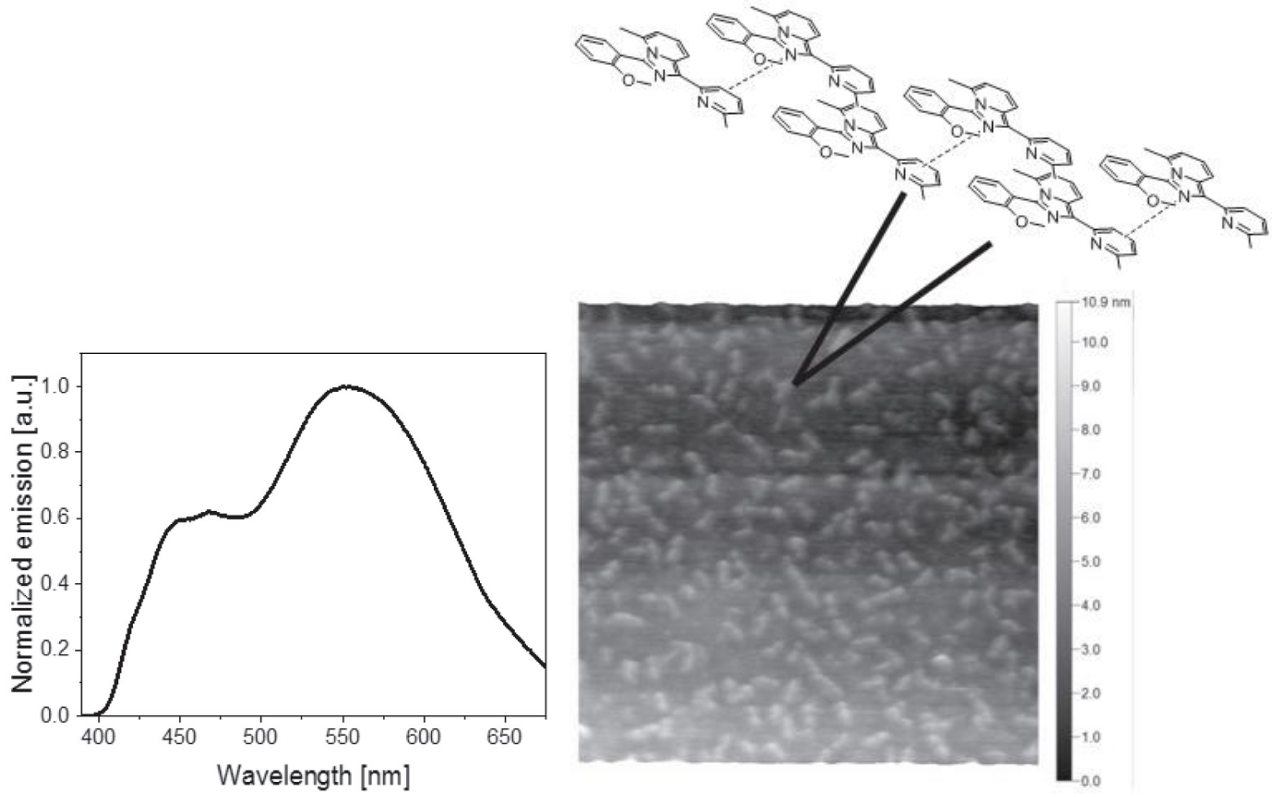

Fig. 6. Photoluminescence spectrum (left), a schematic draw of the aggregates and AFM image (right) of **100** thin films.

3.4. Electroluminescent characterization of Me-impy LECs

Next, we decided to fabricate a series of LECs with **100** films. Prior to the deposition of the active layer, a first layer of poly (3,4-ethylenedioxythiophene):poly(styrenesulfonate) (PEDOT: PSS) (70 nm) was deposited on top of a patterned ITO substrate. The devices were finalized by the physical vapor deposition of 90 nm of aluminum as cathode. The devices were driven at the pulsed current of 15 mA, using a 1000 Hz block-wave and a 50% duty cycle – see experimental section for more details and Table 2 summarizing the device figures-of-merit. These devices show the typical LEC behavior with an initial high voltage of 4.5 V that decays to reach a constant value at 4.3 V. As well, the luminance behavior shows sub-second turn-on times and exponential decay with time. The maximum luminance reached low values of 2.5 cd/m^2 associated to efficiencies of 0.01 cd/A. The electroluminescent response consists of a featureless band centered at 560 nm with a lack of contribution at the high-energy region of the spectrum – Fig. 8. The x/y CIE color coordinates of these devices are 0.42/0.50 indicating that the electroluminescence emission corresponds to orange-emitting devices. This indicates that aggregates emission governs the electroluminescence mechanism, even though both aggregates and monomer species are active under photoexcitate stimuli- vide supra. Quite likely, the aggregates act as electron-hole recombination centers where the emission is produced. Indeed, we also prepared device with **20** films to investigate the electroluminescence response that consisted of a featureless band centered at 480 nm with x/y CIE color coordinates of 0.31/0.41 – Fig. 8 and Table 2. Thus the **20** LEC still does not show any blue response, highlighting the relevance of the presence of aggregates under electrical stimuli of **100** LECs.

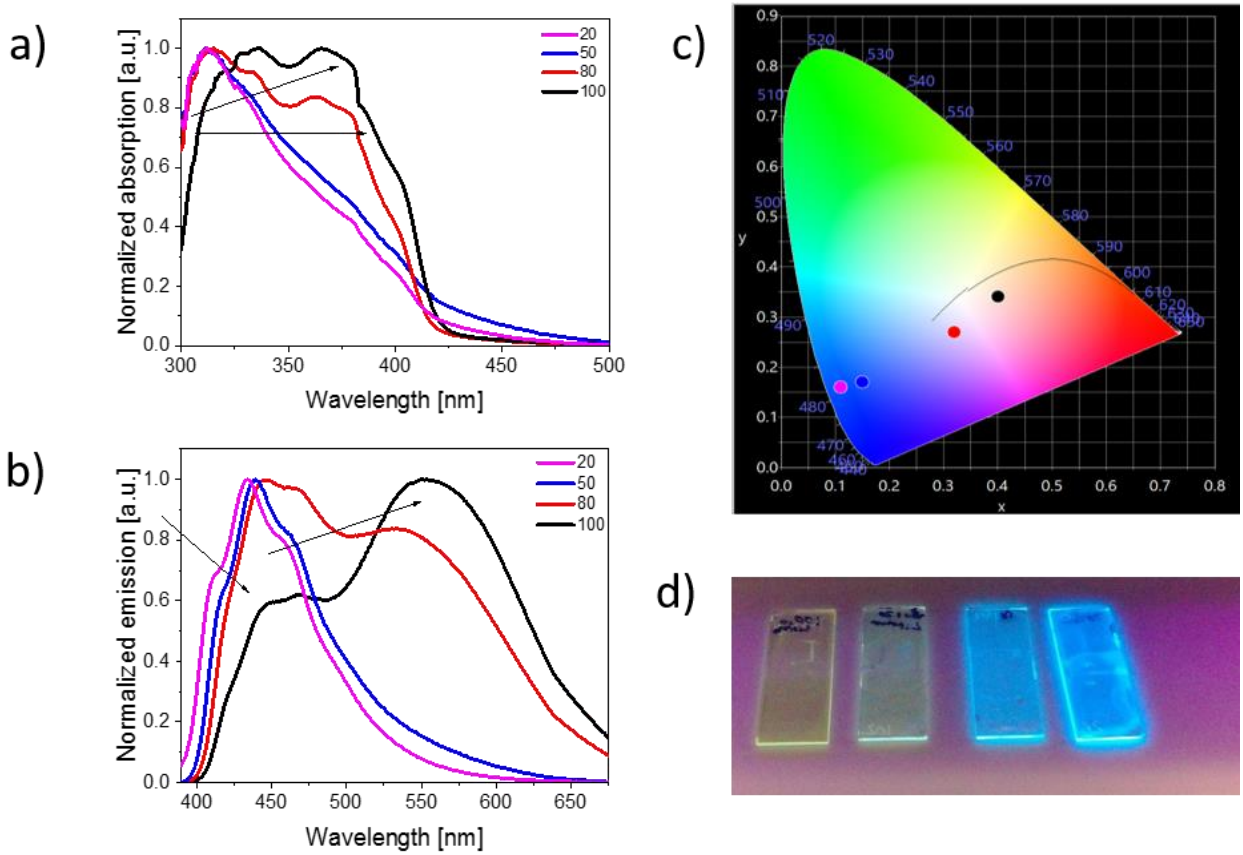

Fig. 7. Absorption (top left) and b) photoluminescence (middle left) of the thin films. c) CIE diagram in which the x/y photoluminescence coordinates of **20** (pink dot), **50** (blue dot), **80** (red dot) and **100** (black dot) are displayed. d) The deposited thin films on ITOs (from left to right, **100**, **80**, **50** and **20**) under a UV lamp (310 nm, 8W).

Table 2. LEC performances of the evaporated devices, measured at the pulsed current of 15 mA.

	Luminance$_{max}$ cd/m^2 [λ_{max} (nm)]	Turn on time s	Lifetime s	Efficacy cd/A	x/y CIE coord.
20	0.3 [540]	0	10	0.001	0.31/0.41
100	2.5 [556]	0	300	0.01	0.42/0.50
Ir(Me-impy)	2.5 [590]	0	900	0.01	0.48/0.52

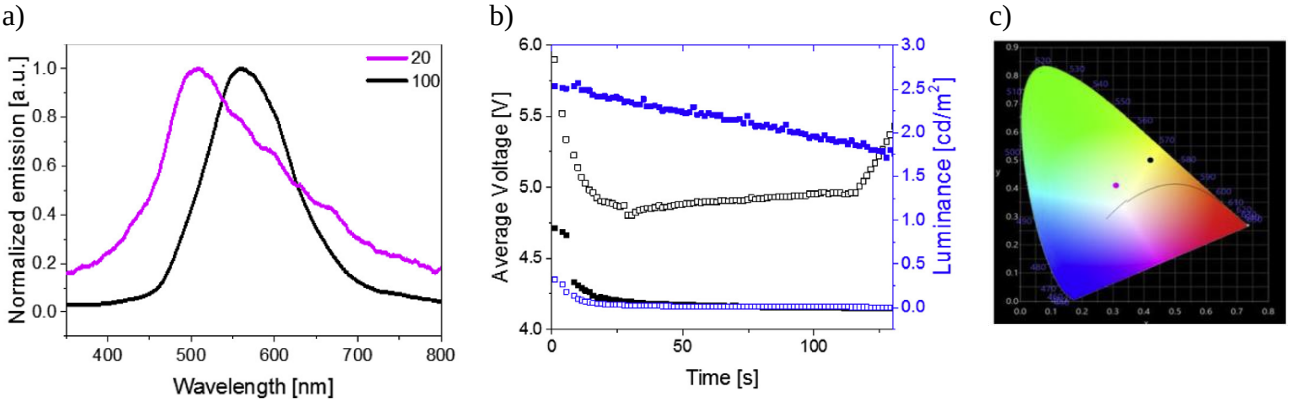

Fig. 8. (a) Normalized electroluminescence spectra of **20** and **100** devices under the driving current of 15 mA. (b) Average Voltage and Luminance versus Time curves under the driving current of 15 mA for the devices **20** (empty squares) and **100** (filled squares). (c) CIE diagram in which the x/y CIE color coordinates of **20** (pink dot) and **100** (black dot) devices are displayed.

3.5. Direct comparison of using Me-impy LECs with those with impy based coordination complexes

In order to contextualize the use of the Me-impy for LECs, we have synthesized the Ir(III) complex $[Ir(ppy)_2(Me\text{-}impy)]PF_6$ (Ir(Me-impy)) and have prepared LECs with this emitter – see experimental section for details. Noteworthy, although Ir(impy) complexes have been reported in the literature, their application for lighting devices has not been explored [63–65]. In brief, the absorption spectrum of Ir(Me-impy) shows an intense UV band located at 260 nm that is ascribed to mixed ligand-centered and metal-to-ligand charge transfer (^{1}LC and ^{1}MLCT, respectively) transitions involving all ligands and a shoulder at 356 nm is assigned to Ir-ppy→ppy singlet transitions – Fig. 9 [63]. The emission features involves a highly structured emission band that is ascribed to the LC phosphorescence nature – Fig. 9 [63]. This is confirmed by the low ϕ (0.05 in degassed acetonitrile solution).

Next, the same device architecture and driving conditions were followed to investigate the electroluminescent response of the Ir(Me-impy) in LECs – see experimental section for details. The device performances are shown in Fig. 10 and the device figures-of-merit are summarized in Table 2. The EL devices show the typical LEC features with a decrease of the voltage after the switch-on until it reaches a steady state at 5.25 V – Fig. 9; the voltage remains approximately constant for more than 4 h, thereby indicating that the emitter is not degrading [3,7]. However, both the maximum luminance (2.4 cd/m^2) and lifetime are quite low compared to other Ir(III) complexes – Fig. 10 [69,70]. More strikingly, the electroluminescence spectrum also consists of a broad shapeless emission band centered at 590 nm that corresponds to a yellow-emitting device (x/y color coordinates of 0.48/0.52) – Fig. 10. This performance is comparable with those using Me-impy, underlining that in this case the use of a metal core is of no use to improve the device performances. This also holds if we directly compare the Me-impy performance with those recently published for LECs with copper(I) complexes bearing this ligand – i.e., luminance of 13.9 cd/m^2, efficacy of 0.028 cd/A, and stability of 0.28 h for a yellow emitting device [58].

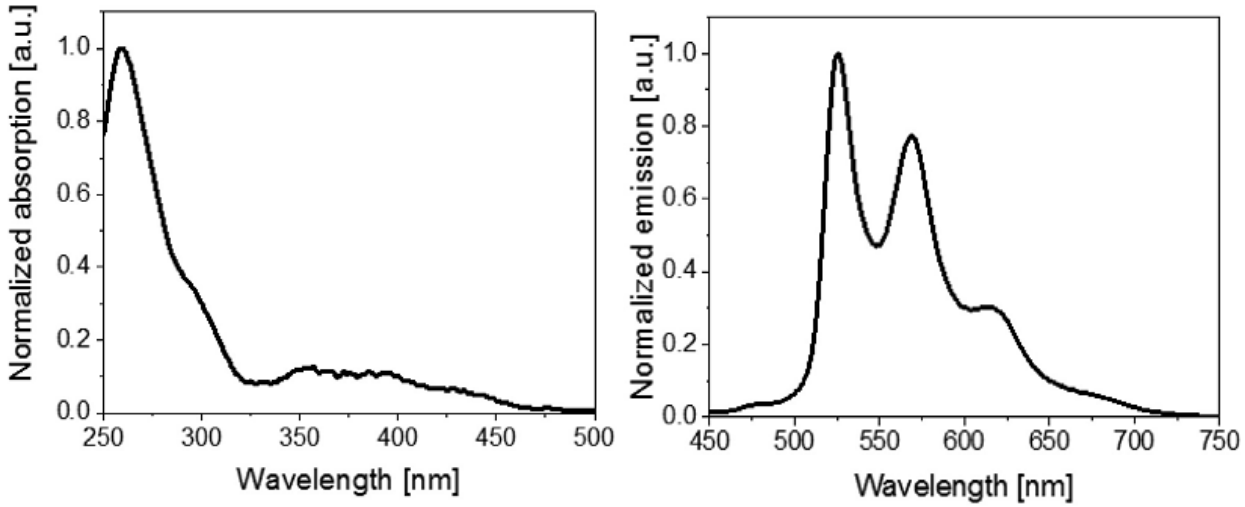

Fig. 9. Absorption (left) and photoluminescence (right) spectra of Ir(Me-impy) in dichloromethane degassed solution.

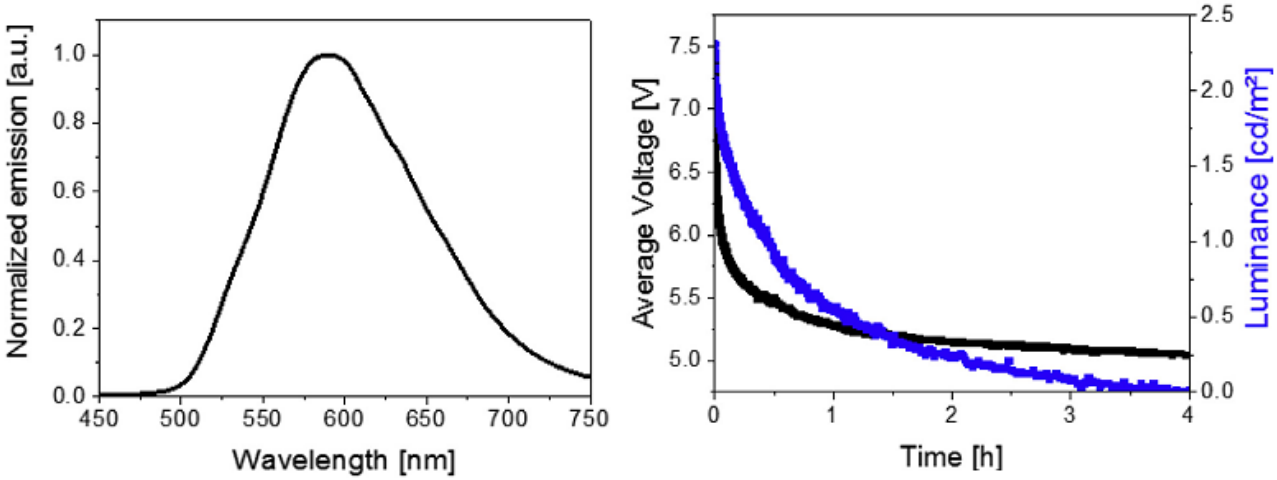

Fig. 10. Electroluminescence spectrum of Ir(Me-impy) (left), recorded under the driving current of 15 mA; Average voltage and Luminance versus Time of an Ir(Me-impy) device (right), at the driving current of 15 mA.

4. Conclusions

A small molecule belonging to the pyrydilimidazo[1,5-a]pyridine family has been for the first time applied in an LEC. This compound is a blue emitter in solution, but it is prone to aggregate in thin films. The aggregation is likely related to a π-π stacking. Here, a deeper study on the tridimensional arrangement needs to be performed to further shed light onto the nature of the aggregates. Although whitish emission is noted per photo-excitation stimuli, the electroluminescence response is described as purely yellow since the aggregates species act as hole/electron recombination species. Even though the EL response is not yet efficient, we contextualize its value with a direct comparison of LECs with Me-impy and Ir(Me-impy) emitters. Both devices feature similar performances, underlining that the use of the expensive metal is in this case of no aid to the enhancement of the figures-of-merit. To conclude, this work, while deeply analyzing the photophysical feature of a pyridilimidazo [1,5-a]pyridine, provides relevant information to further study this family of compounds, towards stable and efficient blue LECs.

Acknowledgments

E.F. and R.D.C. acknowledge the program ‘‘Ayudas para la atracción de talento investigador – Modalidad 1 of the Consejería de Educación, Juventud y Deporte – Comunidad de Madrid with the

reference number 2016-T1/IND-1463". The authors acknowledge Marco Giordano for his help with the synthesis.

References

[1] S. Tang, L. Edman, Top. Curr. Chem. 374 (2016) 40.
[2] E. Fresta, R.D. Costa, J. Mater. Chem. C 5 (2017) 5643.
[3] R.D. Costa, ed., Springer, 2017.
[4] A. Nardelli, E. Deuschle, L.D. de Azevedo, J.L.N. Pessoa, E. Ghisi, Renew. Sustain. Energy Rev. 75 (2017) 368.
[5] L. Edman, The light-emitting electrochemical cell: utilizing ions for self-assembly and improved device operation, in: Funct. Supramol. Arch., Wiley-VCH Verlag GmbH & Co. KGaA, 2011, pp. 895–917.
[6] A.J. Janssen, J. Am. Chem. Soc. 132 (2010) 13776.
[7] S. Van Reenen, T. Akatsuka, D. Tordera, M. Kemerink, H.J. Bolink, J. Am. Chem. Soc. 135 (2013) 886.
[8] R.D. Costa, E. Ortí, H.J. Bolink, Pure Appl. Chem. 83 (2011) 2115.
[9] R.D. Costa, E. Ortí, H.J. Bolink, F. Monti, G. Accorsi, N. Armaroli, Angew. Chemie – Int. Ed. 51 (2012) 8178.
[10] T. Hu, L. He, L. Duan, Y. Qiu, J. Mater. Chem. 22 (2012) 4206.
[11] S.B. Meier, D. Hartmann, A. Winnacker, W. Sarfert, J. Appl. Phys. 116 (2014) 104504.
[12] K.J. Suhr, L.D. Bastatas, Y. Shen, L.A.Mitchell, B.J. Holliday, J.D. Slinker, ACS Appl Mater Interfaces 8 (2016) 8888.
[13] B.M.D. Puscher, M.F. Aygueler, P. Docampo, R.D. Costa, Adv. Energy Mater. 7 (2017) 1602283, https://doi.org/10.1002/aenm.201602283.
[14] M.D. Weber, M. Adam, R.R. Tykwinski, R.D. Costa, Adv. Funct. Mater. 25 (2015) 5066.
[15] M.D. Weber, J.E. Wittmann, A. Burger, O.B. Malcioglu, J. Segarra-Martinez, A. Hirsch, P.B. Coto, M. Bockstedte, R.D. Costa, Adv. Funct. Mater. 26 (2016) 6737.
[16] S. Tang, W.-Y. Tan, X.-H. Zhu, L. Edman, Chem. Commun. 49 (2013) 4926.
[17] K. Sato, S. Uchida, S. Toriyama, S. Nishimura, K. Oyaizu, H. Nishide, Y. Nishikitani, Adv. Mater. Technol. 2 (1600293) (2017) 1.
[18] S. Tang, J. Pan, H.A. Buchholz, L. Edman, J. Am. Chem. Soc. 135 (2013) 3647.
[19] M.F. Aygüler, M.D. Weber, B.M.D. Puscher, D.D. Medina, P. Docampo, R.D. Costa, J. Phys. Chem. C 119 (2015) 12047.
[20] A. Asadpoordarvish, A. Sandström, C. Larsen, R. Bollström, M. Toivakka, R. Österbacka, L. Edman, Adv. Funct. Mater. 25 (2015) 3238.
[21] G. Qian, Y. Lin, G.Wantz, A.R. Davis, K.R. Carter, J.J.Watkins, Adv. Funct. Mater. 24 (2014) 4484.
[22] S. Van Reenen, P.Matyba, A. Dzwilewski, R.A.J. Janssen, L. Edman,M. Kemerink, Adv. Funct. Mater. 21 (2011) 1795.
[23] A. Sandström, L. Edman, Energy Technol. 3 (2015) 329.
[24] G. Mauthner, K. Landfester, A. Köck, H. Brückl, M. Kast, C. Stepper, E.J.W. List, Org. Electron. 9 (2008) 164.
[25] A. Sandström, H.F. Dam, F.C. Krebs, L. Edman, Nat. Commun. 3 (1002) (2012) 1. [26] A. Sandstroem, A. Asadpoordarvish, J. Enevold, L. Edman, Adv.Mater. 26 (2014) 4975.
[27] Z. Zhang, Y. Li, G. Guan, H. Li, Y. Luo, F. Zhao, Q. Zhang, B.Wei, Q. Pei, H. Peng, Z. Zhang, K. Guo, Y. Li, X. Li, G. Guan, H. Li, Y. Luo, F. Zhao, Q. Zhang, B.Wei, Q. Pei, H. Peng, Nat. Photonics 9 (2015) 1.
[28] Z. Zhang, Q. Zhang, K. Guo, Y. Li, X. Li, L. Wang, Y. Luo, H. Li, Y. Zhang, G. Guan, B. Wei, X. Zhu, H. Peng, J. Mater. Chem. C 3 (2015) 5621.

[29] M.S. Subeesh, K. Shanmugasundaram, C.D. Sunesh, R.K. Chitumalla, J. Jang, Y. Choe, J. Phys. Chem. C 120 (2016) 12207.
[30] M.Y.Wong,M.-G. La-Placa, A. Pertegas, H.J. Bolink, E. Zysman-Colman, J. Mater. Chem. C 5 (2017) 1699.
[31] M.Y.Wong, G.J. Hedley, G. Xie, L.S. Kölln, I.D.W. Samuel, A. Pertegás, H.J. Bolink, E. Zysman-Colman, Chem. Mater. 27 (2015) 6535.
[32] P. Lundberg, E.M. Lindh, S. Tang, L. Edman, A.C.S. Appl, Mater. Interfaces 9 (2017) 28810.
[33] M. Elie, F. Sguerra, F. Di Meo, M.D.Weber, R. Marion, A. Grimault, J.F. Lohier, A. Stallivieri, A. Brosseau, R.B. Pansu, J.L. Renaud,M. Linares,M. Hamel, R.D. Costa, S. Gaillard, A.C.S. Appl, Mater. Interfaces 8 (2016) 14678.
[34] C.L. Linfoot, M.J. Leitl, P. Richardson, A.F. Rausch, O. Chepelin, F.J. White, H. Yersin, N. Robertson, Inorg. Chem. 53 (2014) 10854.
[35] H.-F. Chen, C.-T. Liao, T.-C. Chen, H.-C. Su, K.-T.Wong, T.-F. Guo, J. Mater. Chem. 21 (2011) 4175.
[36] H.-F. Chen, C.-T. Liao, M.-C. Kuo, Y.-S. Yeh, H.-C. Su, K.-T. Wong, Org. Electron. 13 (2012) 1765.
[37] K. Shanmugasundaram, M.S. Subeesh, C.D. Sunesh, R.K. Chitumalla, J. Jang, Y. Choe, Org. Electron. Phys. Mater. Appl. 24 (2015) 297–302.
[38] K. Shanmugasundaram, M.S. Subeesh, C.D. Sunesh, R.K. Chitumalla, J. Jang, Y. Choe, J. Phys. Chem. C 120 (2016) 20247.
[39] M.S. Subeesh, K. Shanmugasundaram, C.D. Sunesh, Y.S. Won, Y. Choe, J. Mater. Chem. C 3 (2015) 4683.
[40] S. Kervyn, O. Fenwick, F. Di Stasio, Y.S. Shin, J. Wouters, G. Accorsi, S. Osella, D. Beljonne, F. Cacialli, D. Bonifazi, Chem. – A Eur. J. 19 (2013) 7771.
[41] K.T. Weber, K. Karikis, M.D. Weber, P.B. Coto, A. Charisiadis, D. Charitaki, G. Charalambidis, P. Angaridis, A.G. Coutsolelos, R.D. Costa, Dalton Trans. 45 (2016) 13284.
[42] M.D. Weber, V. Nikolaou, J.E. Wittmann, A. Nikolaou, P.A. Angaridis, G. Charalambidis, C. Stangel, A. Kahnt, A.G. Coutsolelos, R.D. Costa, Chem. Commun. 52 (2016) 1602.
[43] A. Pertegás, D. Tordera, J. Serrano-Pérez, J. Am. Chem. Soc. 135 (2013) 18008, http://pubs.acs.org/doi/abs/10.1021/ja407515w.
[44] A. Pertegas, M.Y. Wong, M. Sessolo, E. Zysman-Colman, H.J. Bolink, ECS J. Solid State Sci. Technol. 5 (2016) R3160.
[45] S. Jenatsch, L. Wang, M. Bulloni, A.C. Véron, B. Ruhstaller, S. Altazin, F. Nüesch, R. Hany, A.C.S. Appl, Mater. Interfaces 8 (2016) 6554.
[46] S. Jenatsch, L. Wang, N. Leclaire, E. Hack, R. Steim, S.B. Anantharaman, J. Heier, B. Ruhstaller, L. Penninck, F. Nüesch, R. Hany, Org. Electron. Phys. Mater. Appl. 48 (2017) 77–84.
[47] A.G. Coutsolelos, A. Charisiadis, A. Bagaki, E. Fresta, K.T. Weber, G. Charalambidis, C. Stangel, A.G. Hatzidimitriou, P.A. Angaridis, R.D. Costa, Chempluschem (2017), https://doi.org/10.1002/cplu.201700416.
[48] K. Shanmugasundaram, M.S. Subeesh, C.D. Sunesh, Y. Choe, RSC Adv. 6 (2016) 28912.
[49] M.Y.Wong,M.-G. La-Placa, A. Pertegas, H.J. Bolink, E. Zysman-Colman, J. Mater. Chem. C 5 (2017) 1699.
[50] G. Horowitz, Adv. Mater. 10 (1998) 365.
[51] K. Singh, R. Boddula, S. Vaidyanathan, Inorg. Chem. 56 (2017) 9376.
[52] P.-T. Chou, Y. Chi, Chem. – A Eur. J. 13 (2007) 380.
[53] G. Volpi, C. Garino, E. Conterosito, C. Barolo, R. Gobetto, G. Viscardi, Dye. Pigment. 128 (2016) 96.
[54] G. Volpi, G. Magnano, I. Benesperi, D. Saccone, E. Priola, V. Gianotti, M. Milanesio, E. Conterosito, C. Barolo, G. Viscardi, Dye. Pigment. 137 (2017) 152.
[55] J. Wang, L. Dyers Jr., R. Mason Jr., P. Amoyaw, X.R. Bu, J. Org. Chem. 70 (2005) 2353.

[56] L. Salassa, C. Garino, A. Albertino, G. Volpi, C. Nervi, R. Gobetto, K.I. Hardcastle, Organometallics 27 (2008) 1427.
[57] C. Garino, T. Ruiu, L. Salassa, A. Albertino, G. Volpi, C. Nervi, R. Gobetto, K.I. Hardcastle, Eur. J. Inorg. Chem. 7 (2008) 3587.
[58] M.D. Weber, C. Garino, G. Volpi, E. Casamassa, M. Milanesio, C. Barolo, R.D. Costa, Dalton Trans. 45 (2016) 8984.
[59] R. Czerwieniec, H. Yersin, Inorg. Chem. 54 (2015) 4322. 136 E. Fresta et al. / Polyhedron 140 (2018) 129–137[60] M. Elie, M.D. Weber, F. Di Meo, F. Sguerra, J.-F. Lohier, R.B. Pansu, J.-L. Renaud, M. Hamel, M. Linares, R.D. Costa, S. Gaillard, Chem. – A Eur. J. (2017), https://doi.org/10.1002/chem.201703270.
[61] R. Czerwieniec, J. Yu, H. Yersin, Inorg. Chem. 50 (2011) 8293.
[62] R. Czerwieniec, M.J. Leitl, H.H.H. Homeier, H. Yersin, Coord. Chem. Rev. 325 (2016) 2.
[63] G. Volpi, C. Garino, L. Salassa, J. Fiedler, K.I. Hardcastle, R. Gobetto, C. Nervi, Chem. – A Eur. J. 15 (2009) 6415.
[64] G. Volpi, C. Garino, C. Nervi, Dalton Trans. 41 (2012) 7098.
[65] G. Volpi, C. Garino, E. Breuza, R. Gobetto, C. Nervi, Dalton Trans. 41 (2012) 1065.
[66] A.M. Blanco-Rodriguez, H. Kvapilova, J. Sykora, M. Towrie, C. Nervi, G. Volpi, S. Zalis, A. Vlcek, J. Am. Chem. Soc. 136 (2014) 5963.
[67] F. Shibahara, R. Sugiura, E. Yamaguchi, A. Kitagawa, T. Murai, J. Org. Chem. 74 (2009) 3566.
[68] F. Shibahara, E. Yamaguchi, A. Kitagawa, A. Imai, T. Murai, Tetrahedron 65 (2009) 5062.
[69] H.J. Bolink, E. Coronado, R.D. Costa, E. Ortì, M. Sessolo, S. Graber, K. Doyle, M. Neuburger, C.E. Housecroft, E.C. Constable, Adv. Mater. 20 (2008) 3910.
[70] D. Ma, T. Tsuboi, Y. Qiu, L. Duan, Adv. Mater. 29 (2017), https://doi.org/10.1002/adma.201603253.